EURASIAN JOURNAL OF MATHEMATICAL AND COMPUTER APPLICATIONS
ISSN 2306–6172
Volume 13, Issue 1 (2025) 26 – 36

CREATION OF AN ALGORITHM FOR ESTIMATION OF CONTACT ANGLES ON TEXTURED SURFACES APPLICABLE FOR MOLECULAR DYNAMICS METHOD

Andryushchenko V. A. [1], **Artishevskii K. V.**, **Solnyshkina O. A.**

Abstract The work is devoted to the construction of an algorithm for calculating the contact angles of droplets, applicable for studying the wettability of various surfaces within the framework of the molecular dynamics method. Existing algorithms for determining contact angles, based on the spherical approximation of spreading drops, give adequate results only for drops with axial symmetry. However, the presence of roughness and textures on surfaces can lead to significant deformations of the droplets and their loss of this symmetry. The proposed algorithm, based on the construction of tangents to drops, makes it possible to carry out adequate estimates of wettability, even for drops that are significantly deformed during spreading. The performance of the proposed algorithm for studying the wettability of metal-graphene composites with various textures deposited on the metal surface is demonstrated. It has been shown that the application of graphene coatings significantly affects not only the values of contact angles, but also the deformation of droplets caused by the textures of metal substrates.

Key words: molecular dynamics, wettability, graphene, texture.

AMS Mathematics Subject Classification: 58J65, 70F35, 76R99, 82C22.

DOI: 10.32523/2306-6172-2025-13-1-26-36

1 Introduction

The study of wettability [1]-[4] at micro- and nanoscales is a current area of research with a wide range of potential applications in various disciplines. In the context of nanotechnology, where size plays a critical role, understanding wettability mechanisms allows the development of innovative nanostructured materials, such as nanoparticles [5], nanocoatings [6] and nanostructured surfaces. This opens up prospects for creating materials with unique properties, such as superhydrophobicity or superhydrophilicity, as well as for the development of micro- and nanodevices. In the field of biomedicine [7]-[8], the study of wettability plays an important role in the development of biomedical materials, implants and biosensors [9]-[10]. Analysis of liquid-surface interactions at micro- and nanoscales contributes to the creation of biocompatible materials, improved cell adhesion [11] to surfaces, and the development of new drug delivery methods. In the field of materials science, the study of wettability helps optimize the characteristics of material surfaces, such as adhesion, corrosion resistance, antibacterial properties,

[1]Corresponding Author.

and others. This facilitates the development of new functional materials with improved properties [12]. In the petrochemical and chemical industries [13], the study of wettability is used to optimize the processes of separation [14], filtration [15] and adsorption [16], which helps to improve the efficiency of production and use of chemical products. Thus, research in the field of wettability at micro and nanoscales is of great importance for various fields of science and technology, contributing to the development of new materials, devices and technologies. The study of wettability is of great importance for understanding and controlling interactions between different materials and fluids. To more effectively control wettability, knowledge of the molecular mechanisms of this process is required. But when studying the mechanisms of wettability, difficulties may arise associated with creating a texture that is uniform over the entire surface area, as well as experimentally measuring the contact angle on the micro- and nanoscales. To solve the above problems, this work proposes to use molecular dynamics simulation. The most common algorithm for calculating the contact angle in molecular dynamics is the sphere approximation algorithm [17]-[18]. Within the framework of the specified algorithm, the contact angle is calculated by describing a sphere around the water and finding the contact angle formed by the approximating sphere and the substrate. However, this algorithm has a number of disadvantages. In order for the approximating sphere to correctly describe the drop, it must have the shape of a spherical segment. In practice, the drops are significantly deformed, which is associated with the complex structure of the surface. Therefore, in some cases it is impossible to construct an adequate spherical approximation. In these cases, the sphere approximation algorithm will produce erroneous results. The purpose of this work is to construct an algorithm that allows adequate determination of the contact angle, even for significantly deformed droplets, as well as to illustrate its applicability for studying the wettability of a system in which droplet deformation can play a significant role. A metal-graphene composite with a texture deposited on the metal surface was chosen for the role of such a system.

2 Modeling

To simulate the wettability of surfaces in this work, the method of classical molecular dynamics was used. Molecular dynamics is a computational method used to model the dynamics of systems of atoms and molecules. Within it, the system under study is modeled at the atomic level, where each atom or molecule is represented as a particle that interacts with other particles in the system. Molecular dynamics simulation was carried out using the LAMMPS software package [19]. The classical method of molecular dynamics is based on solving Newton's equations of motion. There are many different schemes for integrating Newton's equations, varying in speed and accuracy. LAMMPS typically uses the Verlet scheme [20] in high-speed form.

The work considered surfaces consisting of a metal-graphene composite wetted by water droplets. Copper was used as the metal.

The interaction between copper atoms in the substrate was described by the Morse potential [21]

$$U(r) = D_e \left(1 - \exp^{-a(r-r_e)}\right)^2,$$

where r is the distance between particles, D_e is the depth of the potential well, which determines the force of attraction between particles, r_e is the equilibrium distance between particles, a is a parameter that determines the width of the potential well.

To describe the interaction between carbon atoms in graphene, the AIREBO potential was used [22]-[23]

$$U = \frac{1}{2}\sum_{i}\sum_{j\neq i}\left[U_{ij}^{REBO} + U_{ij}^{LJ} + \sum_{k\neq i}\sum_{l\neq i,j,k} U_{kilj}^{TORSION}\right],$$

here U_{ij}^{REBO} - interaction of covalently bonded pairs described by the REBO potential

$$U_{ij}^{REBO} = V_{ij}^{R}\left(r_{ij}\right) + b_{ij}V_{ij}^{A}\left(r_{ij}\right),$$

where V_{ij}^{R} and V_{ij}^{A} вЂ“ are the pair potentials of repulsion and attraction, r_{ij} - is the distance between atoms i and j, b_{ij} - is the value of the bond order, including various chemical effects that affect the strength of interaction of covalent bonds. U_{ij}^{LJ} - is the Lennard-Jones potential multiplied by the switching function, $U_{kilj}^{TORSION}$- is the rotation potential.

$$U_{kilj}^{TORSION} = w_{ki}(r_{ki})w_{ij}(r_{ij})w_{jl}(r_{jl})V^{tors}(\omega_{kijl}),$$

where w is the coupling coefficient between two atoms, V^{tors} is the current rotation potential, ω is the dihedral angle.

In turn, the interaction of carbon and copper atoms with water molecules was specified by the Lennard-Jones potential [24], which describes the van der Waals interaction

$$U(r) = 4\varepsilon\left[\left(\frac{\sigma}{R}\right)^{12} - \left(\frac{\sigma}{R}\right)^{6}\right],$$

where R is the distance between the centers of particles, ε is the depth of the potential well, which determines the force of attraction between particles, and σ is a parameter that determines the equilibrium distance between particles.

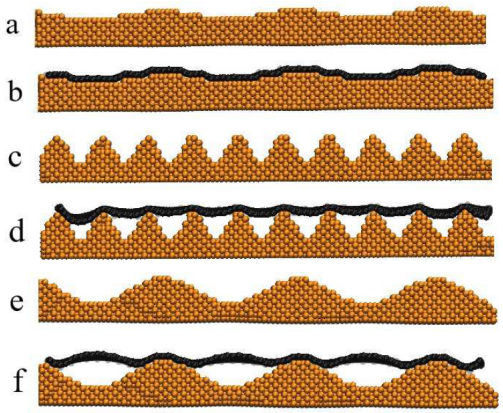

Figure 1: Illustrations of frontal projections of the created surfaces. Cases a, c, e correspond to copper substrates; b, d, f correspond to copper substrates coated with one layer of graphene. For a, b – $\alpha = 2$, $\beta = 60$; for c, d – $\alpha = 6$, $\beta = 20$; for e, f – $\alpha = 6$, $\beta = 60$.

Wetting was carried out with a drop of water. One of the most common models, TIP4P/2005, was used as a model of a water molecule [25]. This is a four-point model of water, which well describes the interaction of water molecules with each other, as well as with the substrate atoms. This circumstance is due to the fact that the oxygen charge is transferred to a separate point M, located on the bisector of the HOH angle at a distance of 0.15Å from the oxygen atom. In this case, the HOH angle is 104.52°. The distances between the hydrogen

atoms and the oxygen atom are 0.9572Å. At the locations of the hydrogen atoms there are charges of $0.52e$, and at point M there is a charge equal to $-1.04e$. This model provides adequate reproduction of the dipole moment of water molecules.

At the initial moment, drops of water in the form of balls were specified above the surface. Their droplet radii were $10 - 12$Å. The simulation was carried out within the framework of the canonical distribution of the thermodynamic system of particles at a temperature of $300°K$. The work examined both atomically smooth and textured surfaces with different numbers of graphene layers. The number of graphene layers varied from zero to three. To create a texture on the substrate, some atoms were removed from the smooth substrate according to the equation $z(x) = \alpha \sin(2\pi x/\beta)$. Parameters α and β specified the amplitude and periodicity of the created texture, respectively. Parameters α and β, like x, have the dimension of length and are measured in angstroms. The length and width of the substrates were approximately 100Å, and the thickness of the substrates was about a dozen atomic layers. Some examples of created surfaces are presented in Figure 1.

3 Algorithm for calculating of contact angle

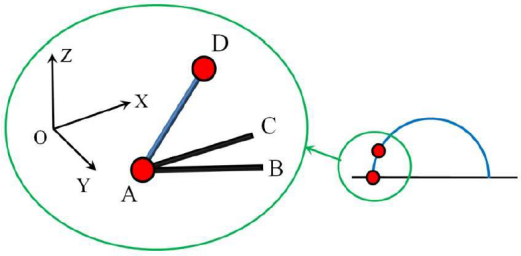

Figure 2: Schematic illustration of constructing a tangent at some point on the contact line of a drop.

To calculate the contact angle when modeling wetting using the molecular dynamics method, algorithms based on the construction of a spherical approximation of droplets are usually used [17]-[18]. The main disadvantage of the "sphere approximation" is that the algorithm produces adequate results only if the drop has the shape of a spherical segment. However, often the drop can have significant deformations due to the presence of roughness and textures on the surfaces. Due to the fact that the above algorithm has significant limitations, the present work discusses the creation, testing and use of an alternative algorithm. In what follows, we will call the created algorithm the tangent algorithm. The essence of this algorithm is to construct tangent lines to a water drop. Since water molecules constantly not only move in space, but also actively rotate, to reduce the fluctuation component, the position of water molecules in the algorithm is associated with the position of oxygen atoms. At the beginning of the algorithm, surface water molecules are clustered into two groups. The first group is obtained by isolating the atoms in contact with the surface of the material. Next, atoms that are also located on the free surface of the drop are selected from this group. To do this, the region occupied by the oxygen atoms of the first group is divided into sectors, after which several atoms are selected from each sector that are maximally distant from point B. Here and below, point B is the projection of the position of the drop center of mass onto the OXY plane (the plane parallel to the base of the substrate). The more sectors are considered, the more accurately the first group of atoms will describe the deformations of the drop.

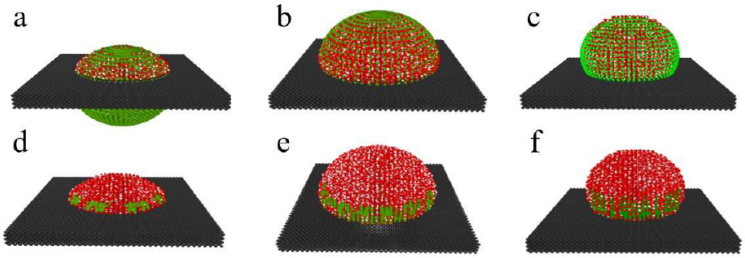

Figure 3: Illustration of testing the algorithm on smooth surfaces. The approximating sphere and tangents are shown in green. For cases a, d - the center of mass of the spherical drop is below the substrate; b, e - center of mass of the droplet on the substrate; c, f - center of mass of the drop above the substrate.

Carrying out these procedures leads to obtaining the coordinates of oxygen atoms on the contact line of the drop. The second group includes all the remaining oxygen atoms on the free surface of the drop. Next, for each atom from the first group, neighboring atoms from the second group are searched. To do this, a sphere with a certain radius is built around each atom from the first group, which makes it possible to select several layers of atoms from the second group. Between neighboring atoms that are potentially suitable for constructing a tangent, a segment AD is constructed (Fig. 2); if the projection of the segment AD onto the OXY plane (segment AC) forms an angle with the segment AB of no more than 10°, then the segment AD is added to the list of tangents.

The segment AB connects the atom in question on the contact line with point B. The angle formed by the segments AD and AB is the desired angle. Using the known coordinates of the beginning and end of the segments, you can find the desired angle from the formula for the scalar product of vectors

$$cos(\theta) = (\mathbf{D} - \mathbf{A})(\mathbf{B} - \mathbf{A})/\big(|\mathbf{D} - \mathbf{A}||\mathbf{B} - \mathbf{A}|\big).$$

The resulting contact angle is calculated as the average of all obtained angles. In addition, unlike the sphere approximation algorithm, the tangent algorithm allows one to obtain information about the distribution of contact angles.

4 Algorithm testing

Testing of the tangent algorithm and its comparison with the sphere approximation algorithm was carried out on smooth (Fig. 3) and textured (Fig. 1) surfaces. In this case, drops with a shape as close as possible to spherical were used.

When considering atomically smooth substrates, the position of the center of mass of the droplets relative to the substrates changed. Thus, droplets with a center of mass position below the substrate, on the substrate, and above it were considered, effectively defining hydrophilic, neutral in wettability, and hydrophobic situations, respectively. The results obtained by the algorithms were compared with the analytical data. On smooth surfaces, the analytical angle was calculated using the equation $\cos(\theta) = 1 - z_0/R$, where R is the radius of the drop, z_0 is the height of the drop above the

substrate, and θ is the contact angle of the drop. On textured surfaces, the analytical angle was calculated using the circular method: the base line was selected, after which the contact angle was calculated as the angle between the tangent and the base line. On smooth surfaces, the sphere approximation algorithm and the tangent algorithm produced results that were close to analytical values. Thus, the analytically calculated angle for cases corresponding to (Fig. 3. a, d) is 58°, for cases (Fig. 3. b, e) - 90°, for cases (Fig. 3. c, f) - 115°. For similar cases, the sphere approximation algorithm produced 60°, 93° and 113°, and the tangent algorithm produced 55°, 87° and 110°, respectively. Thus, the testing results showed that on smooth surfaces, provided that the drop has the shape of a segment of a ball, the sphere approximation algorithm and the tangent algorithm produce results similar to analytical ones, which indicates the correct operation of the algorithms. However, the tangent algorithm also allows you to obtain information not only about the average value of the contact angle, but also the distribution of contact angles (Fig. 4).

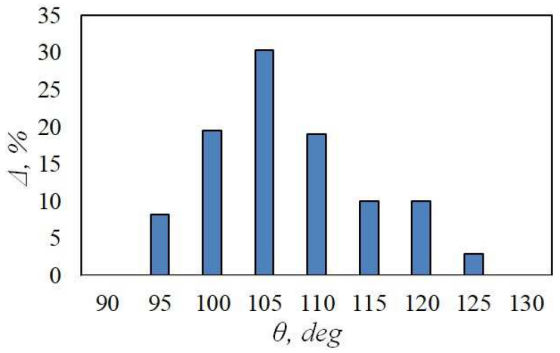

Figure 4: An example of the distribution of angles obtained by the tangent method. The illustration corresponds to drop from Fig. 3, f.

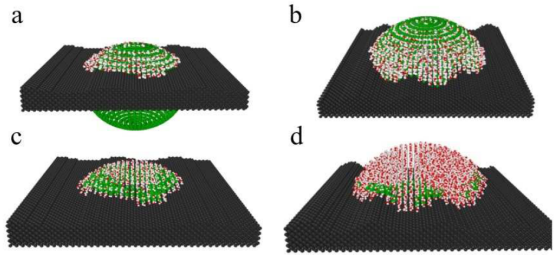

Figure 5: Illustration of testing the algorithm on textured surfaces. The approximating sphere and tangents are shown in green. For cases a, c – $\alpha = 2$, $\beta = 60$; for cases – b, d $\alpha=4$, $\beta=60$. For cases a, b the sphere approximation algorithm was used, and for c, d – the tangent algorithm.

For the case of a drop located above a smooth surface, a certain distribution of angles is observed with an average value consistent with analytical estimates. This distribution for a symmetric droplet is due to the uneven arrangement of atoms in space, caused by the atomic structure of the droplet and the substrate.

On textured surfaces (Fig. 5), the tangent algorithm produces more accurate values θ than the sphere approximation algorithm.

Thus, the analytically calculated angle for the cases (Fig. 5. a, c) is equal to 43°, and for the cases (Fig. 5. b, d) - 60°. For similar cases, the sphere approximation algorithm produced 58° and 80°, and the tangent algorithm 41° and 62°, respectively. Thus, on textured surfaces, even taking into account the fact that the drop is as close as possible to a spherical shape, the contact angle values θ obtained using the sphere approximation algorithm have significant deviations from analytical estimates, in contrast to the tangent algorithm.

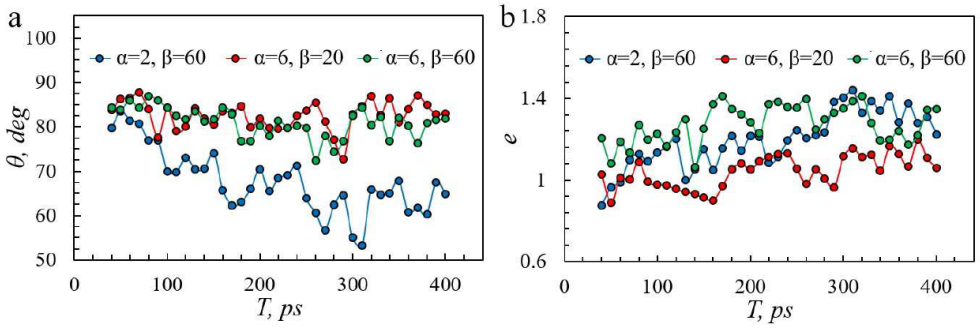

Figure 6: Dependences on time: contact angle – a, and eccentricity – b. Textured surfaces are coated with a single layer of graphene.

5 Results

This section presents the results of modeling the spreading of droplets on metal-graphene composites. Textured substrates were considered, which led to significant deformations of the droplets. In this regard, all the results presented below were obtained using the tangent algorithm. The simulation was carried out until the stationary state of the drop was established, i.e. when the value of the contact angle of the droplets practically did not change, which took about several hundred picoseconds.

On copper substrates without a graphene coating, the material exhibited significant hydrophilicity. Hydrophilicity, naturally, led to a significant influence of the nature of the textures on the values θ of the contact angles. So, for surfaces characterized by $\alpha = 2$, $\beta = 60$ the contact angle is $\theta = 16.5°$, on surfaces with $\alpha = 6$, $\beta = 20$ $\theta = 34°$ and on surfaces with $\alpha = 6$, $\beta = 60$ $\theta = 23°$. The presence of longitudinal textures also led to a loss of droplet symmetry. To describe this effect numerically, we introduce the effective eccentricity - e. Let us define e as the ratio of the maximum linear dimensions of a drop along and across the textures applied to the substrate. Note that the parameter e cannot be directly associated with the classical eccentricity used to describe conic sections. In all the cases considered, significant deformations of the droplets along the surface of the texture substrates were observed. For surfaces characterized by $\alpha = 2$, $\beta = 60$ eccentricity $e = 1.2$, on surfaces with $\alpha = 6$, $\beta = 20$ $e = 1.4$ and on surfaces with $\alpha = 6$, $\beta = 60$ $e = 1.15$. In general, the results when studying the wettability of a copper substrate are consistent with the theoretical and experimental results obtained previously in [26].

The application of even one graphene layer to the surface of copper substrates leads to a significant change in their wettability. Note that in this work, cases of loose adherence of graphene to copper surfaces were considered (Fig. 1). The change in contact angle and effective eccentricity of droplets is presented in Fig. 6.

Stabilization of the contact angles and eccentricities was observed approximately 200 picoseconds after the start of the calculation, which corresponded to the droplets reaching stationary states. These states demonstrated lower hydrophilicity compared to metal surfaces. Thus, for surfaces characterized by $\alpha = 2$, $\beta = 60$, the contact angle and eccentricity are $\theta = 64°$, $e = 1.26$, on surfaces with $\alpha = 6$, $\beta = 20$ $\theta = 82°$, $e = 1.05$ and on surfaces with $\alpha = 6$, $\beta = 60$ $\theta = 81°$, $e = 1.23$. Thus, the change was observed

as both an increase and a decrease in eccentricity compared to copper surfaces. This circumstance is due to the presence of two competing factors. The first factor is the general weakening of the attraction of the copper substrate. The second factor is the unevenness of this weakening due to the uneven adherence of the graphene layer to the surface (Fig. 1).

The application of a second layer of graphene coating leads to a slight increase in the contact angles and a decrease in the eccentricity values. So, for surfaces characterized by $\alpha = 2$, $\beta = 60$, the contact angle and eccentricity are $\theta = 76°$, $e = 1.23$, on surfaces with $\alpha = 6$, $\beta = 20$ $\theta = 80°$, $e = 0.98$ and on surfaces with $\alpha = 6$, $\beta = 60$ $\theta = 81°$, $e = 1$. The observed changes are due to a further weakening of the influence of the copper substrate.

Applying a third layer of graphene coating practically eliminates the influence of the material and texture of the substrate. In this case, the value of the contact angle tends to the value of the graphite contact angle, and the value of the eccentricity tends to unity.

Thus, the presence of textures can lead to a significant violation of the axial symmetry of the drop as it spreads. This effect can be reduced by applying certain smoothing and hydrophobic coatings to the surface (Fig. 7).

Using the effective eccentricity allows us to obtain some information about the deformation of the drop. Significantly more information can be obtained by analyzing the distributions of contact angles obtained by the tangent algorithm. Fig. 8 shows such distributions corresponding to the drops shown in Fig. 7.

For a less deformed drop (Fig. 7 b), the angle distribution had one clearly defined maximum and some deviation from symmetry (Fig. 8 b). For a more deformed drop (Fig. 8 a), the angle distribution had two maximums and a significant deviation from symmetry (Fig. 8 a). Thus, the tangent algorithm allows for a detailed analysis of wettability, in contrast to the sphere approximation algorithm, which produces only a single average value of the contact angle. This circumstance can play a fundamental role if the textures applied to the surface have a more complex appearance than the linear textures considered in the work.

6 Conclusion

As a result of the work, an algorithm was created, tested and applied to calculate the contact angles of droplets to study the wettability of various surfaces within the framework of the molecular dynamics method. In contrast to existing algorithms for determining contact angles, based on the spherical approximation of spreading drops, the created algorithm made it possible to carry out adequate estimates of wettability for drops that significantly deform during spreading. Thus, on surfaces with amplitudes of the created texture of two and four angstroms and a periodicity of sixty angstroms, the analytical estimate gives angle values of 43° and 60°, respectively. For similar cases, the spherical approximation algorithm gives angle values of 58° and 80°, and the tangent algorithm 41° and 62°, respectively. In addition, the proposed algorithm made it possible to calculate and the distribution of contact angles along the contact line of a drop, which made it possible to carry out a more detailed analysis of drops that

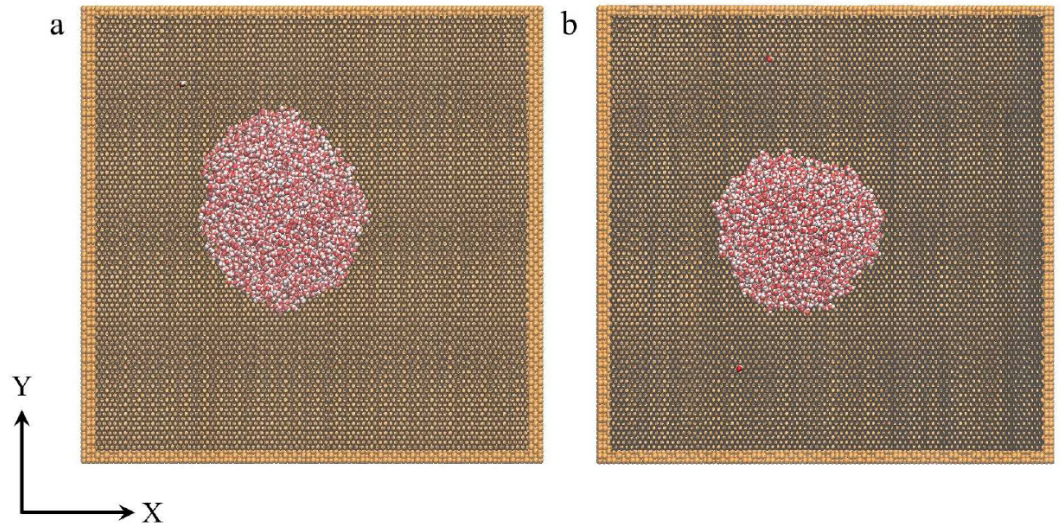

Figure 7: Examples of horizontal projections of droplets spreading over surfaces. For case a – $\alpha = 2$, $\beta = 60$, one layer of graphene is deposited on the surface; for case b – $\alpha = 6$, $\beta = 60$, two layers of graphene are deposited on the surface. The spreading of the drop occurs along the Y axis.

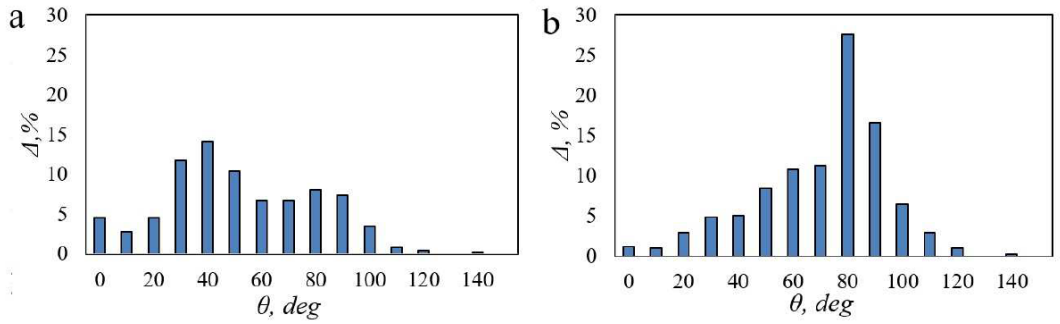

Figure 8: Angle distributions for droplets spreading over surfaces. For the case a - $\alpha = 2$, $\beta = 60$, one layer of graphene is deposited on the surface, $e \sim 1.26$; for case b - $\alpha = 6$, $\beta = 60$, two layers of graphene are deposited on the surface, $e \sim 1$.

significantly deform during spreading. Using the example of surfaces with amplitudes of the created texture of two angstroms and a periodicity of sixty angstroms, covered with one or two layers of graphene, it is shown that the application of a second graphene layer reduces the eccentricity of the droplet from 1.26 to ~ 1. At the same time, the distribution of angles also changes significantly from almost uniform in the range of angles from 0° to 100°, to a distribution with a clearly defined maximum in the region of 80°. It has been shown that when applying graphene coatings, an important factor is not only the number of layers, but also the density of their adjacency to the surface. Using the example of surfaces with a tight fit of one graphene layer to the surface (texture amplitude of two angstroms, texture period of sixty angstroms) and a loose fit of one graphene layer (texture amplitude of six angstroms, texture period of sixty angstroms), a significant difference in the influence of the graphene coating is shown. Thus, the change in the contact angle when applying one graphene layer was $\sim 48°$.

For a surface with a texture amplitude of two angstroms, the angle changed from 16.5° to 64°, and for a surface with a texture amplitude of six angstroms from 34° to 82°. At the same time, the eccentricity for a surface with tight graphene fit changed from 1.2 to 1.26, and for a surface with a less tight fit of graphene from 1.4 to 1.05. The absence of a change in eccentricity with a tighter fit, and its significant change with a loose fit is due to the fact that with a tighter fit of graphene, water droplets feel the copper surface and its texture to a greater extent. Thus, the proposed algorithm allows determine the distributions of droplet contact angles on various textured surfaces, including those modified by coatings, which allows for a more detailed analysis of the state of droplets that are significantly deformed during spreading.

Acknowledgement

The study was financially supported by a grant from the Russian Science Foundation no. 23-29-00260, https://rscf.ru/project/23-29-00260/.

References

[1] Zhao W. et al., *Wettability controlled surface for energy conversion*, Small, 18 (2022), no. 31, 2202906.

[2] Phan H. T. et al., *Surface wettability control by nanocoating: the effects on pool boiling heat transfer and nucleation mechanism*, International Journal of Heat and Mass Transfer, 52 (2009), no. 23-24, 5459-5471.

[3] Macko J. et al., *New insights into hydrophobicity at nanostructured surfaces: Experiments and computational models*, Nanomaterials and Nanotechnology, 12 (2022), 18479804211062316.

[4] Sinha Mahapatra P. et al., *Patterning wettability for open-surface fluidic manipulation: fundamentals and applications*, Chemical reviews, 122 (2022), no. 22, 16752-16801.

[5] Khan S., Hossain M. K., *Classification and properties of nanoparticles*, Nanoparticle-based polymer composites, Woodhead Publishing (2022), 15-54.

[6] Liu S. et al., *Improving surface performance of silicone rubber for composite insulators by multifunctional Nano-coating*, Chemical Engineering Journal, 451 (2023), 138679.

[7] Zhang H. et al., *Janus medical sponge dressings with anisotropic wettability for wound healing*, Applied Materials Today, 23 (2021), 101068.

[8] Li R. et al., *Bioactive materials promote wound healing through modulation of cell behaviors*, Advanced Science, 9 (2022), no. 10, 2105152.

[9] Lindstrom S., Andersson-Svahn H., *Overview of single-cell analyses: microdevices and applications*, Lab on a Chip, 10 (2010), no. 24, 3363-3372.

[10] Polla D. L. et al., *Microdevices in medicine*, Annual review of biomedical engineering, 2 (2000), no. 1, 551-576.

[11] Janiszewska M., Primi M. C., Izard T., *Cell adhesion in cancer: Beyond the migration of single cells*, Journal of biological chemistry, 295 (2020), no. 8, 2495-2505.

[12] Qian L. et al., *Band engineering of carbon nanotubes for device applications*, Matter, 3 (2020), no. 3, 664-695.

[13] Puntervold T. et al., *Adsorption of crude oil components onto carbonate and sandstone outcrop rocks and its effect on wettability*, Energy and Fuels, 35 (2021), no. 7, 5738-5747.

[14] Fan Q. et al., *Bio-based materials with special wettability for oil-water separation*, Separation and Purification Technology, 297 (2022), 121445.

[15] Yang S. et al., *Graphene-based melamine sponges with reverse wettability for oil/water separation through absorption and filtration*, Journal of Environmental Chemical Engineering, 10 (2022), no. 3, 107543.

[16] Ding F., Gao M., *Pore wettability for enhanced oil recovery, contaminant adsorption and oil/water separation: A review*, Advances in Colloid and Interface Science, 289 (2021), 102377.

[17] Fan C. F., Cagin T., *Wetting of crystalline polymer surfaces: A molecular dynamics simulation*, The Journal of chemical physics, 103 (1995), no. 20, 9053-9061.

[18] Do Hong S., Ha M. Y., Balachandar S., *Static and dynamic contact angles of water droplet on a solid surface using molecular dynamics simulation*, Journal of colloid and interface science, 339 (2009), no. 1, 187-195.

[19] Thompson A. P. et al., *LAMMPS-a flexible simulation tool for particle-based materials modeling at the atomic, meso, and continuum scales*, Computer Physics Communications, 271 (2022), 108171.

[20] Verlet L., *Computer "experiments" on classical fluids. I. Thermodynamical properties of Lennard-Jones molecules*, Physical review, 159 (1967), no. 1, 98.

[21] Girifalco L. A., Weizer V. G., *Application of the Morse potential function to cubic metals*, Physical review, 114 (1959), no. 3, 687.

[22] Dhaliwal G., Nair P. B., Singh C. V., *Uncertainty analysis and estimation of robust AIREBO parameters for graphene*, Carbon, 142 (2019), 300-310.

[23] Stuart S. J., Tutein A. B., Harrison J. A., *A reactive potential for hydrocarbons with intermolecular interactions*, The Journal of chemical physics, 112 (2000), no. 14, 6472-6486.

[24] Lennard-Jones J. E., *Cohesion*, Proceedings of the Physical Society, 43 (1931), no. 5, 461.

[25] Gonzalez M. A., Abascal J. L. F., *A flexible model for water based on TIP4P/2005*, The Journal of chemical physics, 135 (2011), no. 22, PAGES.

[26] Andryushchenko V. A., Artishevskii K. V., Smovzh D. V., *Simulation of wettability of nanotextured surfaces by molecular dynamics*, Journal of Applied Mechanics and Technical Physics, 64 (2023), no. 5, 814-820.

Andryushchenko V.A.,
Novosibirsk State University,
Russia, 630090 Novosibirsk, st. Pirogova, 2,
Email: vladimir.andryushchenko@gmail.com,

Artishevskii K.V.,
Novosibirsk State University,
Russia, 630090 Novosibirsk, st. Pirogova, 2,
Email: k.artishevskii@g.nsu.ru,

Solnyshkina O.A.,
Ufa University of Science and Technology,
Russia, 450076 Ufa, st. Zaki Validi, 32,
Email: olgasolnyshkina@gmail.com.

Received 10.08.2024 , Accepted15.01.2025, Available online 31.03.2025.